Solar-Terrestrial Physics. 2025, vol. 11, iss. 2, pp. 60–68. DOI: 10.12737/stp-112202506. © 2025 A.A. Vlasov. Published by INFRA-M Academic Publishing House

DOI: 10.12737/stp-112202506

Received November 25, 2024
Accepted March 24, 2025

STUDYING THE RADIAL STRUCTURE OF THE POLOIDAL ALFVÉN RESONATOR BY THE METHOD OF PHASE PORTRAITS FROM VAN ALLEN PROBES SATELLITE DATA

A.A. Vlasov
Institute of Solar-Terrestrial Physics SB RAS,
Irkutsk, Russia, a.vlasov@mail.iszf.irk.ru

Abstract. In the paper, we examine the spatial structure of eigenharmonics of the poloidal Alfvén resonator recorded by the RBSP-B satellite on 23 October 2012 at 19:12–20:24 UT. We employ the method of phase portraits, which is a set of plots of magnetic/electric field components of oscillations as well as the phase shift between transverse components, to interpret the data. Based on the theoretical description of magnetospheric MHD waves, an analytical solution for eigenharmonics of the poloidal Alfvén resonator is framed. The phase shift of individual harmonics of the observed oscillations is shown to have a quasi-periodic structure, which allows us to confirm that they have resonator modes, and the magnetic field components analytically calculated along the satellite trajectory qualitatively coincide with the satellite data. From comparison of theoretical calculations of the structure of transverse magnetic field components with observational data, we put forward an assumption that the second and fourth harmonics of the poloidal resonator make the main contribution to the observed oscillations.

Keywords: Alfvén waves, poloidal resonator, ULF waves, satellite observations.

INTRODUCTION

Alfvén waves, one of the branches of magnetohydrodynamic plasma oscillations, play a significant role in the dynamics of the magnetosphere [Keiling, 2009]. Their spatial structure is diverse and depends on properties of the medium and the wave source. It is customary to distinguish two types of polarization of Alfvén waves. Waves with a dominant radial (across magnetic shells) magnetic field component is called poloidal. Such waves are azimuthally small-scale, i.e., their azimuthal wavenumber $m \gg 1$ [Leonovich, Mazur, 1993]. Sources of such waves can be ionospheric currents or resonant interaction with charged plasma particles [Leonovich, Mazur, 1996; Lee, Lysak, 1990]. Waves dominated by the azimuthal magnetic field component are called toroidal and they are usually azimuthally large-scale $(m \sim 1)$. Generation of toroidal oscillations is more often associated with field line resonance (FLR) [Tamao, 1965; Chen, Hasegawa, 1974; Southwood, 1974].

An important plasma characteristic in studying Alfvén waves is the Alfvén velocity distribution, defined in the Gaussian unit system as $v_A = B/\sqrt{4\pi\rho}$, where B is the magnetic field strength; ρ is the mass plasma density. In the transition region between the outer and inner magnetosphere, called the plasmapause, due to a sharp decrease in plasma concentration in the direction across magnetic shells [Kim et al., 2018], the Alfvén velocity distribution has two local extremes (minimum and maximum). In these regions, Alfvén resonators can be formed — regions bounded transversely by turning points, and longitudinally (along magnetic field lines) by the conductive ionosphere, in which standing waves trapped inside can be generated and maintained [Leonovich, Mazur, 1995].

It is worth noting that wave confinement can also occur in other regions of near-Earth space [Lysak, Yoshikawa, 2006]. The Schumann resonance in the Earth—ionosphere system is well known. It plays an important role in monitoring global electrical phenomena, such as thunderstorm activity [Schumann, 1952]. The ionospheric Alfvén resonator (IAR), which is formed inside the ionosphere between its base and the region above the F-layer maximum, has been thoroughly studied [Polyakov, Rapoport, 1981]. Finally, resonators for ion-cyclotron and ion-ion hybrid modes can also be formed in the magnetosphere. In the longitudinal direction, such waves are trapped between reflecting points near the geomagnetic equator [Guglielmi et al., 2001; Mikhailova et al., 2020].

Satellite observations of Alfvén waves in the magnetosphere have been conducted for several decades. Missions such as CLUSTER, Van Allen Probes, THEMIS, and others make it possible to detect Alfvén oscillations inside the magnetosphere; for example, in the frequency range from a few to several tens of millihertz (Pc4-Pc5), the fundamental (first) or second harmonics of the standing poloidal mode are generally recorded [Min et al., 2017; Takahashi et al., 2018]. Nevertheless, Alfvén waves have a diverse small-scale transverse structure that has not yet been studied in detail by satellites [Stasiewicz et al., 2000]. The main problem in determining the spatial structure of magnetohydrodynamic waves is the fact that satellite measurements are time series of

physical parameters related to the satellite's position in space. This causes difficulties in trying to unambiguously separate temporal and spatial variations, which hinders the determination of the spatial wave structure. This problem is partially solved by grouping four or more instruments [Paschmann, Daly, 2008].

To identify the small-scale radial (across magnetic shells) structures of monochromatic Alfvén oscillations from data obtained by one instrument, Leonovich et al. [2022] have proposed a phase portrait method. The phase portrait of Alfvén wave is a set of plots of magnetic (or electric) wave field components and the phase shift between transverse magnetic (or electric) wave field components. For a monochromatic wave, this value does not depend on time, azimuthal, and longitudinal coordinates, which makes it possible to unambiguously determine the transverse structure and type of Alfvén oscillations from single-satellite data. Kozlov et al. [2024], using the phase portrait method, have first studied the spatial Alfvén wave structure when polarization changes from poloidal to toroidal. In this paper, we examine the observation of eigenharmonics of the poloidal Alfvén resonator formed in the vicinity of a local maximum of the Alfvén velocity [Mager et al., 2018].

The work has the following structure. The first section describes the results of observations by the Van Allen Probes satellite (RBSP-B), which on October 23, 2012 at 19:12–20:12 UT recorded Alfvén oscillations in a region presumably being the poloidal Alfvén resonator. Next, using the phase portrait method, we analyze the behavior of the phase shift between the transverse magnetic field components of individual quasi-monochromatic harmonics. The second section presents basic equations describing the spatial structure of poloidal resonator harmonics, and expressions employed in analytical calculations of the field structure. The third section compares satellite data with analytical calculations of the structure of eigenharmonics of the poloidal resonator. In conclusion, the main results of the study are formulated.

1. SATELLITE OBSERVATIONS

According to [Mager et al., 2018], on October 23, 2012 at 19:12–20:24 UT, RBSP-B detected an ultralow-frequency wave with dominant harmonics of 13.6 and 15.3 mHz. This case is considered as the first observation of the transverse Alfvén resonator in Earth's magnetosphere. This conclusion was made by the authors from several factors: 1) during the event, the satellite crossed the region of maximum of the distribution of Alfvén oscillation eigenfrequencies, and it is in this region that the poloidal resonator can be formed in a finite pressure plasma; 2) according to analytical estimates, the poloidal eigenfrequency turned out to be higher than the toroidal frequency, which is also a condition for forming the poloidal resonator in the region of maximum; 3) several adjacent frequency harmonics were found.

The wave source is proton bump-on-tail instability at ~80 keV. The wave propagated westward, and its azimuthal wave number m=–100.

Figure 1 displays plots for different spatial parameters of the satellite taken directly from the data. A change is shown in the McIlwain parameter along the trajectory of the satellite that moved into the magnetosphere. The *MLT* value, given in degrees and hours, indicates that the satellite was in the dawn sector. Finally, a change in the magnetic latitude *MLAT* is shown from which it follows that the satellite practically did not shift in latitude during the event.

Figure 2 exhibits amplitudes of the magnetic field components, as well as their corresponding wavelet spectra. For the analysis, data has been used from the EMFISIS magnetometer in the GSE (Geocentric Solar Ecliptic) coordinate system with an interval of 4 s, to which a bandpass filter with 3 and 40 mHz boundaries was applied. The background magnetic field B_0 was determined using the moving average method. Then, projections of the perturbed magnetic field were found in the coordinate system related to the field line geometry: longitudinal — in the direction of the background magnetic field $\mathbf{e}_\parallel = \mathbf{B}_0 / |\mathbf{B}_0|$, azimuthal — in the direction $\mathbf{e}_\phi = \mathbf{e}_\parallel \times \mathbf{r} / r$, where $\mathbf{r}$ is the radius vector of the satellite location, and radial — in the direction $\mathbf{e}_r = \mathbf{e}_\phi \times \mathbf{e}_\parallel$. In general, $\mathbf{e}_r \neq \mathbf{r} / r_\parallel$.

The wavelet spectrum and the magnetic field components suggest that the amplitudes of the azimuthal and radial components are approximately equal and significantly exceed the amplitude of the longitudinal (compressional) component. This is a characteristic feature of the Alfvén wave. Throughout the event, ~8 min beats are observed in the spectrum of the radial and azimuthal components, which indicates the presence of

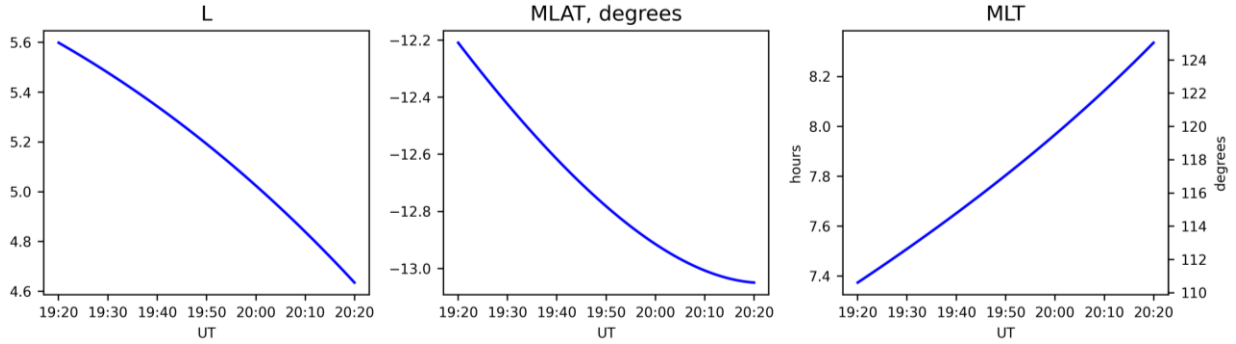

Figure 1. Parameters related to the location of RBSP-B during the event: *a* — a change in the McIlwain parameter during the event; *b* — magnetic latitude in degrees (*MLAT*); *c* — local magnetic time *MLT* given in hours (left axis) and degrees (right axis)

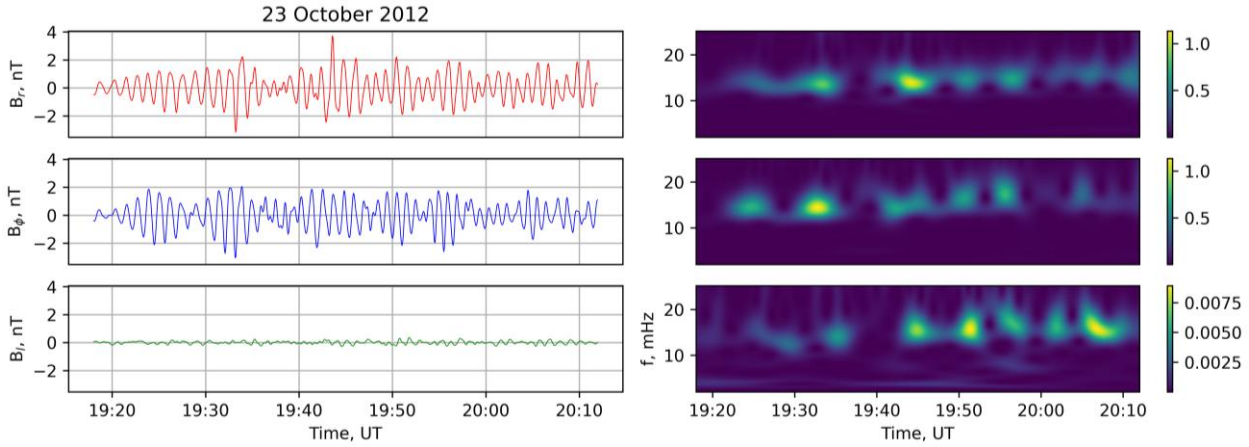

Figure 2. Magnetic field components in a coordinate system linked to magnetic field lines (*a*): the radial field component B_r (across magnetic shells, red curve), the azimuthal component B_ϕ (blue curve), the longitudinal component B_l directed along magnetic field lines (green curve). The Morlet wavelet spectrum normalized to the response of a single signal (*b*). At the top is the spectrum of the radial magnetic field component B_r; in the center is the spectrum of the azimuthal magnetic field component B_ϕ; at the bottom is the spectrum of the longitudinal magnetic field component B_l

several close harmonics and is one of the signs of the presence of a transverse resonator.

For a more visual representation of the dominant frequencies in the event, Figure 3 shows the spectral signal power density, where both peaks in the vicinity of 13.6 and 15.3 mHz are clearly seen in both transverse magnetic field components. In addition to them, other peaks can be observed in each component, but their amplitudes are much smaller.

Figure 4 illustrates initial oscillations of the radial and azimuthal components of the perturbed magnetic field and the sum of the monochromatic components identified by a narrowband Butterworth filter with center frequencies of 13.6 and 15.3 mHz and a half-width of 1 mHz.

Applied implementation of the filter involves double filtering, which makes it possible to compensate for possible phase distortions.

Let us use the phase portrait method proposed in [Leonovich et al., 2022] to verify the assumption that observed oscillations are harmonics of the poloidal Alfvén resonator. In the coordinate system related to the magnetic field, the expression for the phase shift in the transverse components has the form

$$\Delta_\varphi = \operatorname{arctg}\frac{\operatorname{Im}\left(B_\phi / B_r\right)}{\operatorname{Re}\left(B_\phi / B_r\right)} \pm \pi n, \quad n = 0, 1, 2 \ldots \qquad (1)$$

A similar expression is derived for the electric field components. The addition $\pm\pi n$ occurs naturally due to properties of the function arctg and is necessary to construct a smooth graph without discontinuities. Analytical expression (1) is obtained for a complex-valued analytical solution. The phase of the observed quasi-monochromatic signal can also be determined using different algorithms, noteworthy among which is the construction of an analytical signal via the Hilbert transform. This method of identifying the signal amplitude and phase has proven itself well in studies of geomagnetic pulsations [Glassmeier, 1980; Cramm et al., 2000; Eriksson et al., 2006].

To construct an analytical signal $w(t)$ of an arbitrary time series $u(t)$, we use the Hilbert transform [Wakman, Weinstein, 1977]

$$w(t) = u(t) + \frac{i}{\pi}\int_{-\infty}^{\infty}\frac{u(s)\,ds}{t-s} = A(t)e^{i\Phi(t)}, \qquad (2)$$

where $u(t)$ is the original time series; $A(t)$ is the signal amplitude; $\Phi(t)$ is the signal phase that can be used to build a phase portrait.

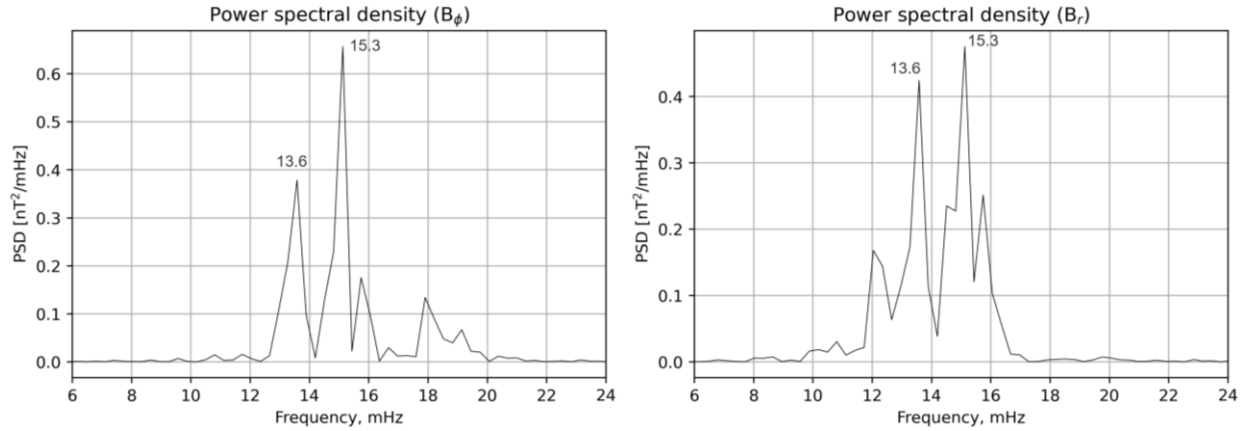

Figure 3. Spectral power density (SPD) for transverse magnetic field components B_ϕ and B_r

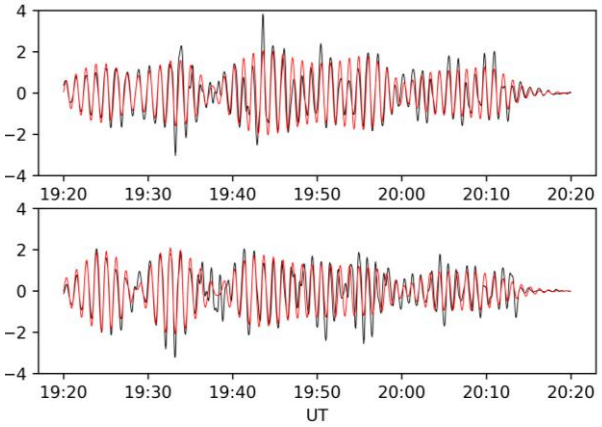

Figure 4. Perturbed transverse magnetic field components B_r and B_ϕ (black lines) and the sum of the selected monochromatic components corresponding to spectral density peaks (red lines)

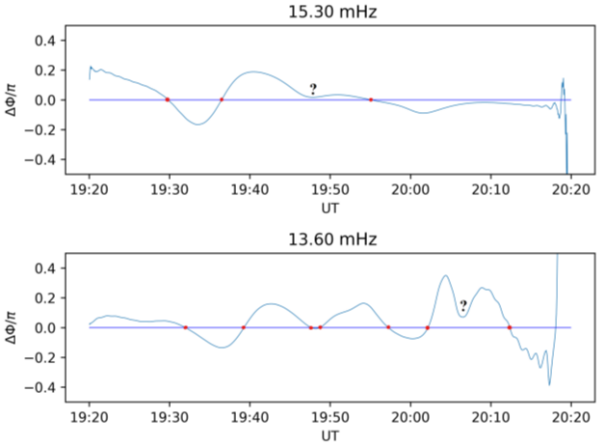

Figure 5. Phase shift constructed for the 15.3 and 13.6 mHz harmonics from satellite data. The harmonics were identified using a narrowband filter. Red dots mark transitions of phase difference through zero, which are taken into account in the calculation. The question mark indicates regions exhibiting phase difference fluctuations that do not cross zero.

Figure 5 depicts the phase shift for the selected quasi-monochromatic harmonics obtained from satellite data. It is easy to see that the phase difference for both harmonics is a sign-changing function, which, in general, corresponds to the behavior of the phase difference for resonator modes. Leonovich et al. [2022] have shown that the phase difference between the transverse electric/magnetic field components of the poloidal Alfvén resonator harmonic ranges from $-\pi/2$ to $\pi/2$. In this case, the number of zero crossings is $2n+1$, where n is the resonator harmonic number.

Note that the maximum amplitudes of the phase difference in Figure 4 are lower than $\pi/2$, but the vibrational structure is quite noticeable. As for the number of zero crossings (sign changes), for the 15.3 mHz harmonic their number is 3, which corresponds to the harmonic $n=1$, and for 13.6 mHz, the number of crossings is 7 ($n=3$). The places where the sign is changed are marked with red dots. Transitions located at the end of the interval are ignored since they are associated with the edge effects of the Hilbert transform. Nonetheless, there are phase oscillations on the plots (indicated by a question mark) that do not cross zero. It is difficult to say whether it is necessary to take them into account for the number of intersections. If we assume that such intersections would occur, oscillations with a frequency of 15.3 mHz would correspond to $n=2$ (5 intersections), and for 13.6 mHz the number of transitions would be 9 ($n=4$).

Such discrepancies in the behavior of the observed phase shift with the model difference constructed within the framework of the theoretical resonator model can be attributed to various reasons. First of all, the phase shift can be affected by the presence of small oscillations in the filtered harmonics with frequencies close to the central ones, which do not form standing waves. Note that the phase shift for Alfvén waves traveling across magnetic shells is zero or has a multiple of π. It is unfortunately impossible to identify the contribution of individual quasi-monochromatic signal components neither in phases of the magnetic field components nor in their shift. Note also that the model phase shift is constructed for the resonator's eigenharmonics. However, in the real magnetosphere, eigenoscillations of the transverse resonator should settle after excitation, i.e., form standing harmonics. Moreover, Alfvén waves in the magnetosphere can lose their energy, for example, due to ohmic heating of the ionosphere [Southwood, Kivelson, 2001]. If the attenuation is great enough, it can also hinder the formation of the resonator's standing harmonics and change the behavior of the phase shift between the magnetic field components.

Nevertheless, harmonic phase shift feature an oscillatory structure, which differs fundamentally from the case described in [Kozlov et al., 2024]. The authors have examined the generation of poloidal Alfvén waves on neighboring shells in the vicinity of the local maximum of eigenfrequency distribution, with the phase shift of the transverse components varying monotonously from $-\pi/2$ to $3\pi/2$ over the entire measurement range. Thus, analysis of the phase shift in this case allows us to confirm the resonatory nature of the observed oscillations, yet it can hardly serve as a strict indicator for determining the ordinal number of poloidal resonator modes.

Next, we will construct an analytical description of the spatial structure of the poloidal resonator's eigenharmonics, which can be compared with the structure of the observed oscillations.

2. ANALYTICAL DESCRIPTION OF THE POLOIDAL ALFVÉN RESONATOR

In Earth's magnetosphere, each magnetic shell has its own eigenfrequency of Alfvén oscillations that depends on plasma parameters. At the same time, there is a region in the vicinity of the plasmapause in which the Alfvén velocity and eigenfrequencies have two extremes (minimum and maximum). It is in such regions that the transverse resonator can theoretically exist [Leonovich, Mazur, 1990]. How-

ever, this requires that the poloidal Ω_{PN} and toroidal Ω_{TN} eigenfrequencies differ significantly from each other. It has been found that the polarization splitting of the spectrum (the difference between the poloidal Ω_{PN} and toroidal Ω_{TN} eigenfrequencies) in the dipole magnetic field is large enough only for the fundamental harmonic.

In the cold plasma approximation $(\beta \ll 1)$, $\Omega_{TN} > \Omega_{PN}$. Then, the transverse resonator for azimuthally small-scale waves $(m \gg 1)$ can be formed only at the minimum of the distribution of poloidal eigenfrequencies located inside the plasmapause when the transparency region is between two poloidal resonant surfaces (Figure 6, *a*). Klimushkin et al. [2004] have shown that the polarization splitting of the spectrum directly depends on plasma pressure distribution across magnetic shells. In a finite-pressure plasma, a more likely case is $\Omega_{PN} > \Omega_{TN}$ [Mager, Klimushkin, 2013]. Then, the resonator may appear at the maximum of eigenfrequency distributions near the outer plasmapause (see Figure 6, *b*).

To describe the spatial structure of MHD oscillations, it is convenient to use an orthogonal curvilinear coordinate system (x^1, x^2, x^3), where x^1 is the radial component directed across magnetic shells; x^2 is the azimuthal coordinate; x^3 is the field-aligned coordinate.

Monochromatic MHD oscillations depending on x^2 can be represented as an expansion in harmonics of the form $\sim e^{-i\omega t + i k_2 x^2}$, where $k_2 = m$ is the azimuthal wave vector when $x^2 = \phi$. The homogeneous equation describing the structure of Alfvén waves with $m \gg 1$ has the form [Leonovich, Mazur, 1993]

$$\left[\nabla_1 \hat{L}_T(\omega) \nabla_1 - k_2^2 \hat{L}_P(\omega)\right] \varphi = 0, \tag{3}$$

where $\nabla_1 \equiv \partial / \partial x^1$; φ is the scalar potential describing the Alfvén wave field. Expressions for the toroidal and poloidal operators $L_T(\omega)$ and $L_P(\omega)$ are defined as

$$\hat{L}_T = \frac{\partial}{\partial l} p \frac{\partial}{\partial l} + p \frac{\omega^2}{v_A^2}, \quad \hat{L}_P = \frac{\partial}{\partial l} p^{-1} \frac{\partial}{\partial l} + p^{-1} \frac{\omega^2}{v_A^2}, \tag{4}$$

where $p = \sqrt{g_2 / g_1}$; v_A is the Alfvén velocity; g_1, g_2, g_3 are metric tensor components. The derivatives are taken with respect to the physical length of magnetic field lines $l\left(dl = \sqrt{g_3}\, dx^3\right)$. The transverse magnetic field components in such a coordinate system are expressed through the potential φ:

$$B_1 = \frac{c}{\omega} \frac{g_1}{\sqrt{g}} k_2 \nabla_3 \varphi, \quad B_2 = i \frac{c}{\omega} \frac{g_2}{\sqrt{g}} \nabla_1 \nabla_3 \varphi, \tag{5}$$

where c is the speed of light; $g = g_1 g_2 g_3$.

When the longitudinal wavelength is much longer than the transverse wavelength, the method of different scales can be applied to problem (3). This makes it possible to reduce the two-dimensional problem to the successive solution of longitudinal and transverse problems. In this case, we are looking for a solution in the form of a product of two functions, with U depending only on the transverse coordinate x^1 and describing the small-scale structure of the wave across magnetic shells, and P describing the large-scale longitudinal Alfvén wave structure in the direction x^3:

$$\varphi = U\left(x^1\right) P\left(x^1, x^3\right). \tag{6}$$

By definition, there is a relation near the poloidal surface

$$\left|\frac{\nabla_1}{\sqrt{g_1}}\right| \ll \frac{k_2}{\sqrt{g_2}} \tag{7}$$

and the first term in Equation (3) proves to be much smaller than the second, so it can be discarded in the main order of the perturbation theory. As a result, the longitudinal problem has the form

$$\hat{L}_P(\omega) \varphi = 0, \; \varphi|_{l\pm} = 0, \tag{8}$$

where the boundary condition is written for a perfectly conducting ionosphere.

The solution of problem (8) is a set of eigenfrequencies Ω_{PN} and eigenharmonics P_N. In the WKB approximation, the solution of the longitudinal problem in the form $\hat{L}_P P_N = 0$ is as follows

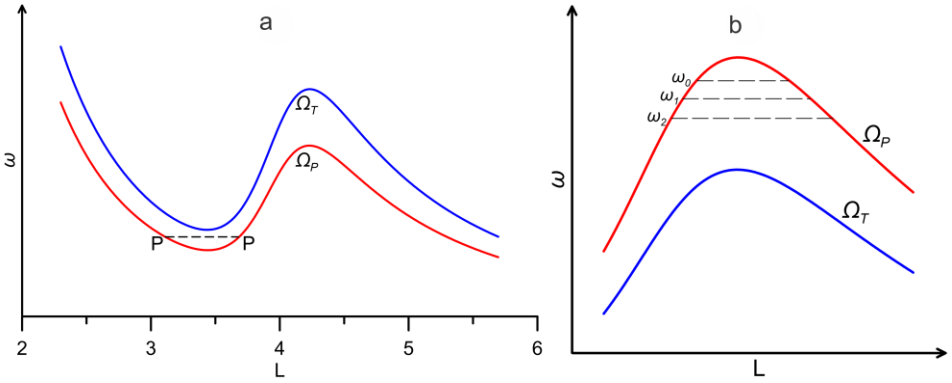

Figure 6. Typical distribution of toroidal and poloidal eigenfrequencies across magnetic shells in the cold plasma approximation (*a*). Blue and red curves represent the toroidal and poloidal eigenfrequencies. The black dashed line between two P points is a possible region of resonator formation between poloidal surfaces. Schematic distribution of the toroidal and poloidal eigenfrequencies in the vicinity of the maximum in the finite-pressure plasma approximation (*b*). Black dashed lines are examples of the poloidal resonator's harmonics with frequencies ω_0, ω_1, and ω_2.

$$P_N = \left(\frac{p v_A}{t_A} \right)^{1/2} \sin\left(\frac{\pi N}{t_A} \int_{l_-}^{l} \frac{dl'}{v_A} \right), \quad (9)$$

where t_A is the Alfvén wave travel time between magnetoconjugate ionospheres; N is the number of the longitudinal harmonic.

The equation for U_N describing the transverse wave structure with $m \gg 1$ was obtained in [Leonovich, Mazur, 1993]:

$$w_N^P \nabla_1^2 U_N + k_2^2 \left[\left(\omega^2 + i\gamma_N \right)^2 - \Omega_{PN}^2 \right] U_N = k_2^2 I_N, \quad (10)$$

where I_N is the multiplier responsible for the external source, for example, ionospheric currents; γ_N is the attenuation decrement, and w_N^P is defined as

$$w_N^P = \frac{1}{t_A} \int_{l_-}^{l_+} v_A \, pp'' dl. \quad (11)$$

Introduce a dimensionless variable $\zeta = (a - a_{PN}) / \lambda_{PN}$, where a_{PN} is the position of the maximum in the distribution of poloidal eigenfrequencies; λ_{PN} is the characteristic radial scale of the solution. In this case, dimensionless equation (10) takes the form

$$\frac{d^2 U_N}{d\zeta} + \left(\sigma - \zeta^2 \right) U_N = \frac{a_{PN}^2 I_\parallel}{\lambda_{PN}^2 \omega}, \quad (12)$$

where

$$\sigma = \frac{a_{PN}^2}{\lambda_{PN}^2} \frac{\left(\omega + i\gamma_N \right)^2 - \Omega_{PN}^2}{\omega^2}. \quad (13)$$

If there are no extraneous currents in the ionosphere (we assume this since eigenoscillations can be formed in the poloidal resonator without an external source), the right-hand side of Equation (12) vanishes. In this case, a well-known quantum oscillator problem is obtained. Its solution [Leonovich, Mazur, 1995]:

$$U_N = C_N y_n(\zeta), \; \sigma = \sigma_n = 2n + 1, \quad (14)$$

where

$$y_n(\zeta) = \frac{1}{\pi^{1/4} 2^{n/2}} \frac{1}{n!^{1/2}} e^{-\zeta^2/2} H_n(\zeta), \quad (15)$$

$H_n(\zeta)$ is Hermite polynomials.

As a result, the scalar potential φ describing the Alfvén wave structure with a frequency ω and an azimuthal wavenumber m is defined as

$$\varphi\left(x^1, \phi, x^3, t \right) = A_n P_N\left(x^1, x^3 \right) y_n e^{-i\omega t + im\phi}, \quad (16)$$

where A_n is the generalized normalization coefficient.

Before we move on to comparing analytical results with observational data, let us talk about limitations of this comparison. Solution (16) is constructed under the assumption that the structure of the resonator harmonics along field lines is common to the entire resonator and has the form of standing longitudinal harmonics P_N. This assumption is acceptable when considering oscillations that are rather narrowly localized across field lines. The same applies to using the parabolic profile for squared eigenfrequency — for an arbitrary function this expansion is applicable only in the immediate vicinity of the extremum. As shown in Figure 1, in the observation interval of interest, the satellite recorded Alfvén oscillations on shells L=4.6÷5.6, which corresponds to the width of the resonator region in the equatorial region ~R_E, with the lengths of dipole magnetic field lines differing by a factor of 1.2 at the beginning and at the end of the interval. We can therefore expect only a qualitative correspondence of the structure of the analytical solutions to the structure of the observed harmonics of the transverse resonator.

3. ANALYTICAL CALCULATIONS

To theoretically calculate the field structure in this event, expressions obtained from Formula (5) have been used. The magnetic field components are expressed in terms of the functions P_N and y_n:

$$B_r = \sum\nolimits_n A_n y_n \frac{im}{a} \frac{\partial P_N}{\partial l} e^{-i\omega_n t + im\phi}, \quad (17)$$

$$B_\phi = \sum\nolimits_n A_n \frac{\partial y_n}{\partial a} \frac{\partial P_N}{\partial l} e^{-i\omega_n t + im\phi}. \quad (18)$$

The poloidal operator eigenfunctions P_N, as well as the resonator eigenharmonics y_n are plotted in Figure 7.

Referring to Figure 3, the 13.6 and 15.3 mHz harmonics have comparable amplitudes. Further, in numerical calculations, the amplitudes of both reference frequencies in the spectrum are considered equal $A_{15.3}$=$A_{13.6}$. For the azimuthal number, we use the estimate m=–100 obtained in [Mager et al., 2018].

The function $y_n(\zeta)$ depends on the dimensionless parameter ζ. Its value depends on the coordinate a of the satellite's position and on the characteristic scale of the solution λ_{PN}. As follows from (17)–(18), the amplitude ratio $|B_r| / |B_\phi| \approx (m/a) l$, where l is the typical scale of change in y_n. Fugure 3 shows that the amplitudes of the radial and azimuthal components are approximately equal, so we can expect that $\lambda_{PN} \sim l \sim L_0/m$, where L_0 is the position of the center of the resonator. In further calculations, we employ the following values of the parameters: $L_0 \approx 5.2\ R_E$, $\lambda_{PN} \approx L_0/45 \approx 730$ km. As a result, the parameter λ_{PN} is selected in such a way that the ratio between amplitudes of the radial and azimuthal magnetic field components approximately matches the observed ones; and the radial scale of the solution, the scale of the observed oscillations.

Find the physical value of the magnetic field components by taking the real part of (17)–(18). For the magnetic field of the harmonic n of the transverse resonator, we have

$$B_{rn} = \frac{m}{a} y_n \frac{\partial P_N}{\partial l} \left[A_n \cos\left(m\phi - \omega_n t + \frac{\pi}{2} \right) \right], \quad (19)$$

$$B_{\phi n} = \frac{\partial y_n}{\partial a} \frac{\partial P_N}{\partial l} \left[A_n \cos\left(m\phi - \omega_n t \right) \right]. \quad (20)$$

Now compare the spatial structure of the observed monochromatic harmonics of the poloidal resonator with the

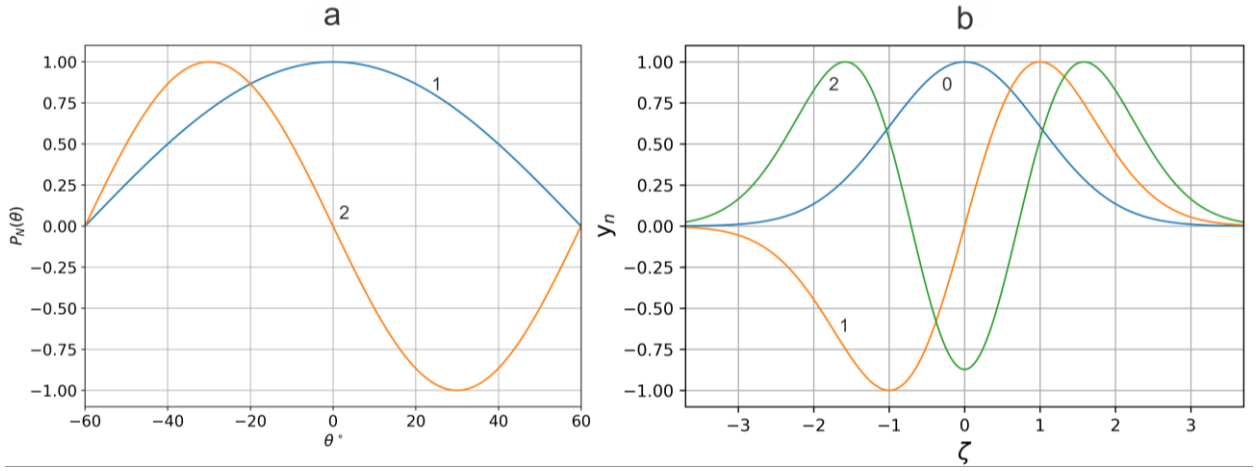

Figure 7. Poloidal eigenfunctions P_N for the first two harmonics n=1, 2 (*a*); resonator eigenfunctions γ_n for the first three harmonics n=0, 1, 2 (*b*)

analytical solutions calculated along the satellite trajectory. Figure 8 shows azimuthal components of individual magnetic field harmonics B_ϕ. Mager et al. [2018] have assumed that the 15.3 mHz harmonic corresponds to the resonator mode n=0; and 13.6 mHz, to n=2. The analysis of the phase difference between monochromatic harmonics has suggested that these are higher resonator modes. The red curves enveloping the harmonics n=2 for the 15.3 mHz and n=4 for 13.6 mHz fit best the observations. As part of the study, analytical solutions were constructed for other eigenharmonics n, but the behavior of their envelopes showed the worst fit to observations. For example, we can compare the analytical solution for n=2 (red curve in the top panel) with the 13.6 mHz harmonic envelope (blue curve at the bottom) to make sure that it corresponds much worse to the observation than the solution for n=4 (bottom panel).

The behavior of the envelopes (bold curves) of the 15.3 mHz harmonic, i.e. the location of amplitude distribution peaks and the radial scale, proves to be quite similar for the observations and analytical solutions. For a higher harmonic corresponding to the frequency of 13.6 mHz, we can also see a similarity between arrangements of the envelope amplitude peaks, but the amplitude of the observed component gradually decreases by the end of the interval.

It has to be said the assumption made in [Mager et al., 2018] that the harmonics n=0 and n=2 were observed also included estimated resonant eigenfrequencies of Alfvén oscillations. For this purpose, a simplified version of the formula for resonator frequencies from [Mager, Klimushkin, 2013] was used. In full, the formula has the form

$$\omega_n^2 = \Omega_{PN}^2 + \frac{1}{2}\left(a\Omega_{PN}\right)^2\left(2n+1\right)^2 - \\ -\frac{1}{2}\left(a\Omega_{PN}\right)^2\left(2n+1\right)^2\sqrt{1+4\frac{\Omega_{PN}^2-\Omega_{TN}^2}{\left(a\Omega_{PN}\right)^2\left(2n+1\right)^2}}, \quad (21)$$

where $a=L_0/(m\Delta L)$, where ΔL is the half-width of the resonator, which for the case in question can be estimated as $\Delta L=0.4R_E$ [Mager et at, 2018]. Assuming that $\Omega_{TN}=\alpha\Omega_{PN}$, we rearrange Formula (21) in the form

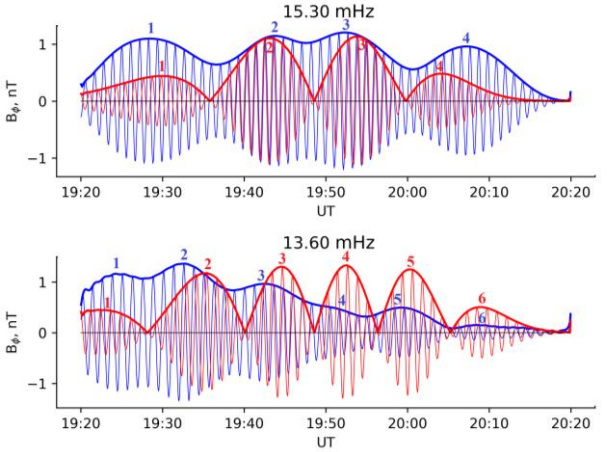

Figure 8. Azimuthal magnetic field component B_ϕ. The blue curve is the component selected by a narrowband filter from satellite data; the red curve is the component constructed using an analytical solution. Numbers indicate local maxima of envelopes

$$\frac{\omega_n^2}{\Omega_{PN}^2} = 1+\frac{1}{2}a^2\left(2n+1\right)^2 - \\ -\frac{1}{2}a^2\left(2n+1\right)^2\sqrt{1+4\frac{1-\alpha^2}{a^2\left(2n+1\right)^2}}. \quad (22)$$

From the resulting expression, we can find the parameter α for an arbitrary ratio between the resonator harmonic frequencies $\omega_{n1}^2/\omega_{n2}^2$, and then restore the poloidal frequency and its associated toroidal frequency.

For ω_0=15.3 mHz, ω_2=13.6 mHz, we get Ω_{PN}=15.95 mHz, Ω_{TN}=11.9 mHz, which is in complete agreement with the estimates [Mager et al, 2018]. For ω_2=15.3 mHz, ω_4=13.6 mHz, we obtain Ω_{PN}=19.2 mHz, Ω_{TN}=10.9 mHz. The polarization splitting of the spectrum, which can be defined as the ratio of the difference between eigenfrequencies to their half-sum, becomes quite large in the case of harmonics 2 and 4 and amounts to 0.55, whereas for 0 and 2 it is smaller, but also quite large and approximately equal to 0.29. In cold plasma, the fundamental harmonic of Alfvén eigenoscil-

lations has the largest spectral splitting and it did not exceed 0.2 [Leonovich, Mazur, 1993; Kozlov, Leonovich, 2006]. Klimushkin et al. [2004] have estimated eigenfrequencies in the plasma approximation with the kinetic pressure gradient. It appeared that when the poloidal frequency becomes higher than the toroidal frequency, polarization splitting can be much larger than that in cold plasma (0.5) and depends on medium parameters.

Note that this result was obtained exclusively from magnetic field measurements, which greatly simplifies the analysis. Electric field measurements, on the contrary, are often less stable, subject to various deviations, require additional calibration, or are often completely unavailable [Breneman et al, 2022]. Thus, this method allows us to qualitatively study the spatial structure of a wave, using data from a single instrument.

CONCLUSION

The main results of this work are as follows.

1. We have analyzed satellite data for the first case of observing harmonics of the poloidal Alfvén resonator, using the phase portrait method. The phase shift between individual quasi-monochromatic harmonics in this case is demonstrated to have a quasi-periodic structure, which is qualitatively consistent with the analytical model of the resonator and suggests that the observed oscillations are indeed harmonics of the resonator.

2. We have compared analytical solutions, based on the theory of the poloidal Alfvén resonator, with magnetic field measurement data from RBSP-B. It is shown that the analytical solutions for the second and fourth harmonics of the poloidal resonator respectively are in best agreement with the transverse structure of the 15.3 and 13.6 mHz harmonics.

3. The comparison of the analytical magnetic field components with RBSP-B data and the analysis of the behavior of the phase difference allowed us to assume that the main contribution to Alfvén oscillations, observed by RBSP-B on October 23, 2012 at 19:12–20:24 UT, was most likely made by the second and fourth harmonics of the poloidal Alfvén resonator. The results indicate the possibility of determining the type of Alfvén waves and analyzing their radial structure by using data from even one spacecraft.

I thank the reviewer A.G. Demekhov for his valuable comments that greatly improved the article. I am grateful to the NASA Van Allen Probes mission team and Craig Kletzing for providing access to EMFISIS data, as well as to D.A. Kozlov, D.Yu. Klimushkin, and P.N. Mager for useful discussions.

The work was financially supported by RSF (Grant No. 22-77-10032).

REFERENCES

Breneman A.W., Wygant J.R., Tian S., Cattell C.A., Thaller S.A., Goetz K., et al. The Van Allen Probes Electric Field and Waves Instrument: Science Results, Measurements, and Access to Data. *Space Sci. Rev*. 2022, vol. 218, no. 8, article id. 69. DOI: 10.1007/s11214-022-00934-y.

Chen L., Hasegawa A. A theory of long-period magnetic pulsations: 1. Steady state excitation of field line resonance. *J. Geophys. Res*. 1974, vol. 79, pp. 1024–1032.

Cramm R., Glassmeier K.H., Othmer C., Fornacon K.H., Auster H.U., Baumjohann W., Georgescu E. A case study of a radially polarized Pc4 event observed by the Equator-S satellite. *Ann. Geophys*. 2000, vol. 18, no. 4, pp. 411–415.

Eriksson P.T.I., Walker A.D.M., Stephenson J.A.E. A statistical correlation of Pc5 pulsations and solar wind pressure oscillations. *Adv. Space Res.* 2006, vol. 38, no. 8, pp. 1763–1771.

Glassmeier K.H. Magnetometer array observations of a giant pulsation event. *J. Geophys. Zeitschrift Geophysik*. 1980, vol. 48, no. 3, pp. 127–138.

Guglielmi A.V., Kangas J., Potapov A.S. Quasiperiodic modulation of the Pc1 geomagnetic pulsations: An unsettled problem. *J. Geophys. Res.: Space Phys.* 2001, vol. 106, no. A11, pp. 25847–25855. DOI: 10.1029/2001JA000136.

Keiling A. Alfvén Waves and Their Roles in the Dynamics of the Earth's Magnetotail: A Review. *Space Sci. Rev.* 2009, vol. 142, pp. 73–156.

Kim K.-H., Kim G.-J., Kwon H.-J. Distribution of equatorial Alfven velocity in the magnetosphere: A statistical analysis of THEMIS observations. *Earth Planets and Space*. 2018, vol. 70, no. 1, p. 174. DOI: 10.1186/s40623-018-0947-9.

Klimushkin D.Y., Mager P.N., Glassmeier K.H. Toroidal and poloidal Alfvén waves with arbitrary azimuthal wavenumbers in a finite pressure plasma in the Earth's magnetosphere. *Ann. Geophys*. 2004, vol. 22, no. 1, pp. 267–287. DOI: 10.5194/angeo-22-267-2004.

Kozlov D.A., Leonovich A.S. Polarization splitting of the Alfvén wave spectrum in a dipole magnetosphere with a rotating plasma. *Plasma Physics Rep*. 2006, vol. 32, no. 9, pp. 765–774.

Kozlov D.A., Leonovich A.S., Vlasov A.A. Determining the radial structure of high-m Alfvén wave by means of the "phase portrait" method. *Adv. Space Res*. 2024, vol. 73, no. 1, pp. 624–631.

Lee D.H., Lysak R.L. Effects of azimuthal asymmetry on ULF waves in the dipole magnetosphere. *Geophys. Res. Lett.* 1990, vol. 17, no. 1, pp. 53–56.

Leonovich A.S., Mazur V.A. The spatial structure of poloidal Alfvén oscillations of an axisymmetric magnetosphere. *Planetary and Space Science*. 1990, vol. 43, pp. 1231–1241. DOI: 10.1016/0032-0633(90)90128-D.

Leonovich A.S., Mazur V.A. A theory of transverse small-scale standing Alfven waves in an axially symmetric magnetosphere. *Planetary and Space Science*. 1993, vol. 41, pp. 697–717.

Leonovich A.S., Mazur V.A. Magnetospheric resonator for transverse-small-scale standing Alfven waves. *Planetary and Space Science*. 1995, vol. 43, pp. 881–883.

Leonovich A.S., Mazur V.A. Penetration to the Earth's surface of standing Alfvén waves excited by external currents in the ionosphere. *Ann. Geophys*. 1996, vol. 14, pp. 545–556.

Leonovich A.S., Zong Q.-Z., Kozlov D.A., Vlasov A.A. "Phase portraits" of Alfvén waves in magnetospheric plasma. *J. Geophys. Res.: Space Phys.* 2022, vol. 127, no. 6, p. e2022JA030432.

Lysak R.L., Yoshikawa A. Resonant cavities and waveguides in the ionosphere and atmosphere. *Magnetospheric ULF Waves: Synthesis and New Directions.* Eds. K. Takahashi, P.J. Chi, R.E. Denton, R.L. Lysak. Washington, American Geophysical Union, 2006, vol. 169, pp. 289–306. DOI: 10.1029/169GM19.

Mager P.N., Klimushkin D.Yu. Giant pulsations as modes of a transverse Alfvénic resonator on the plasmapause. *Earth, Planets and Space*. 2013, vol. 65, pp. 397–409. DOI: 10.5047/eps.2012.10.002.

Mager P.N., Mikhailova O.S., Mager O.V., Klimushkin D.Yu. Eigenmodes of the transverse Alfvénic resonator at the plasmapause: A Van Allen Probes case study. *Geophys. Res. Lett*. 2018, vol. 45, no. 19, pp. 10796–10804. DOI: 10.1029/2018GL079596.

Mikhailova O.S., Mager P.N., Klimushkin D.Yu. Transverse resonator for ion-ion hybrid waves in dipole magnetospheric plasma. *Plasma Physics and Controlled Fusion*. 2020, vol. 62, no. 9, p. 095008. DOI: 10.1088/1361-6587/ab9be9.

Min K., Takahashi K., Ukhorskiy A.Y., Manweiler J.W., Spence H.E., Singer H.J., et al. Second harmonic poloidal waves observed by Van Allen Probes in the dusk-midnight sector. *J. Geophys. Res.: Space Phys*. 2017, vol. 122, pp. 3013–3039.

Paschmann G., Daly P.W. Multi-spacecraft analysis methods revisited. *International Space Science Institute*. 2008, 100 p.

Polyakov S.V., Rapoport V.O. Ionosfernyj al'fvenovskij resonator. *Geomagnetizm i aeronomiya*[Geomagnetism and aeronomy]. 1981, vol. 21, no. 5, pp. 610–614. (In Russian).

Schumann W.O. Über die strahlungslosen Eigenschwingungen einer leitenden Kugel, die von einer Luftschicht und einer Ionosphärenhülle umgeben ist. *Zeitschrift für Naturforschung A*. 1952, vol. 7, no. 2, pp. 149–154. DOI: 10.1515/zna-1952-0202.

Southwood D.J. Some features of field line resonances in the magnetosphere. *Planetary and Space Science*. 1974, vol. 22, pp. 483–491.

Southwood D.J., Kivelson M.G. Damping standing Alfvén waves in the magnetosphere. *J. Geophys. Res*. 2001, vol. 106, pp. 10829–10836.

Stasiewicz K., Bellan P., Chaston C., Kletzing C., Lysak R., Maggs J., et al. Small Scale Alfvénic Structure in the Aurora. *Space Sci. Rev*. 2000, vol. 92, pp. 423–533.

Takahashi K., Oimatsu S., Nosé M., Min K., Claudepierre S.G., Chan A., et al. Van Allen Probes observations of second-harmonic poloidal standing Alfvén waves. *J. Geophys. Res.: Space Phys*. 2018, vol. 123, pp. 611–637.

Tamao T. Transmission and coupling resonance of hydromagnetic disturbances in the non-uniform Earth's magnetosphere. *Science Reports of Tohoku University*. 1965, vol. 17, pp. 43–54.

Vakman D.E., Vajnshtejn L.A. Amplituda, faza, chastota — osnovnye ponyatiya teorii kolebanij. *Uspekhi fizicheskih nauk* [Advances in the physical sciences]. 1977, vol. 123, no. 4, pp. 657–682. (In Russian).

Original Russian version: Vlasov A.A., published in Solnechno-zemnaya fizika. 2025, vol. 11, no. 2, pp. 69–78. DOI: 10.12737/szf-112202506.

How to cite this article

Vlasov A.A. Studying the radial structure of the poloidal Alfvén resonator by the method of phase portraits from Van Allen Probes satellite data. *Sol.-Terr. Phys*. 2025, vol. 11, iss. 2, pp. 60–68. DOI: 10.12737/stp-112202506.